

## Aharonov-Bohm Excitons at Elevated Temperatures in Type-II ZnTe/ZnSe Quantum Dots

I. R. Sellers,<sup>1,\*</sup> V. R. Whiteside,<sup>1</sup> I. L. Kuskovsky,<sup>2</sup> A. O. Govorov,<sup>3</sup> and B. D. McCombe<sup>1</sup>

<sup>1</sup>*Department of Physics, Fronczak Hall, University at Buffalo SUNY, Buffalo, New York 14260, USA*

<sup>2</sup>*Department of Physics, Queens College of CUNY, Flushing, New York 10031, USA*

<sup>3</sup>*Department of Physics & Astronomy, Ohio University, Athens, Ohio 45701, USA*

(Received 23 October 2007; revised manuscript received 13 February 2008; published 3 April 2008)

Optical emission from type-II ZnTe/ZnSe quantum dots demonstrates large and persistent oscillations in *both* the peak energy *and* intensity indicating the formation of coherently rotating states. Furthermore, these Aharonov-Bohm oscillations are shown to be remarkably robust and persist until 180 K. This is at least one order of magnitude greater than the typical temperatures in lithographically defined rings. To our knowledge, this is the highest temperature at which the AB effect has been observed in solid-state and molecular nanostructures.

DOI: [10.1103/PhysRevLett.100.136405](https://doi.org/10.1103/PhysRevLett.100.136405)

PACS numbers: 71.35.Ji, 78.55.Et, 78.67.Hc, 85.35.Be

The Aharonov-Bohm (AB) effect describes a phase shift induced upon a charged particle as it orbits a magnetic flux in a closed trajectory [1]. Due to recent progress in epitaxial growth and device fabrication techniques, the AB effect has now been demonstrated in metallic and semiconductor ring geometries in magneto-transport measurements [2–4], and for self-assembled quantum rings (QR) by far-infrared and capacitance methods [5], and magnetization spectroscopy [6]. Recently, an interesting question has arisen concerning the possibility of observing the AB effect in neutral composite particles such as excitons, and in particular, if it is possible to observe AB oscillations in the optical properties of ringlike nanostructures. The AB effect is a property of charged particles; nevertheless, there have been several theoretical predictions [7–11] concerning mechanisms leading to AB oscillations for neutral excitons. One mechanism [8–11] suggests strong AB oscillations since the electron and hole in a ringlike nanostructure move over different trajectories resulting in a nonzero electric dipole moment. Type-II quantum dots (QDs) have been predicted to be particularly amenable to exhibiting such AB effects because of enhanced polarization of the composite particles due to the spatial separation of the electron and hole in such systems [8,10,11].

The AB effect in QRs/QDs is predicted to have significant effects upon the luminescence properties of the nanostructures since, due to the cylindrical symmetry of the confinement, the exciton ground state has zero orbital angular momentum projection ( $L = 0$ ) at zero magnetic field, but changes to states of higher orbital angular momentum (projection) ( $L = -1, -2, -3$ ) with increasing magnetic field. As a result, the ground state energy oscillates as the  $L$  states cross, and the intensity changes from strong (bright excitonic transition with  $L = 0$ ) to weak (dark excitonic transitions for states with  $L \neq 0$ ) with increasing magnetic field [8,11]. Until now, the AB effects predicted to be observable in the emission have not been seen in *both* the energy *and* intensity in a single QD/QR structure. Although AB oscillations in the emission energy

have been observed in (InGa)As QRs [12] and type-II InP/GaAs QDs [13], analogous effects have not been observed in the PL intensity. In very recent work, a single AB oscillation in the *intensity* was observed [14], but oscillations in the luminescence *energy* were not reported. The recent demonstrations of the optical AB effect [12–14] suggest an interesting possibility to modulate the emission of QDs, which may have potential applications in quantum information systems [15,16].

We report strong simultaneous AB oscillations in *both* the emission *energy* and *intensity* from a single structure. In addition, we have investigated the temperature dependence of the PL and find that the AB oscillations are remarkably robust against temperature, with the signature of the AB effect visible up to 180 K. This is a much higher temperature than reported for lithographically-defined structures. Even in *smaller* lithographically-defined rings with dimensions of a few hundreds of nanometers, the temperature at which the AB effect disappears is about 10 K [4]. Interestingly, the maximum temperature observed in our type-II confined structures is even higher than that observed for carbon nanotubes (CN) ( $\sim 70$  K) [17], which typically have much smaller radii. In general, the AB effect in a QR exists if the QR circumference is shorter than, or comparable to, the phase-coherence length. In CNs, the phase-coherence length of carriers might be reduced by the effect of the surface, which is not a problem in our nanostructures since they are embedded deeply in a crystalline matrix.

The sample studied is a 240 layer ZnTe/ZnSe structure grown by molecular beam epitaxy. Although the growth details are described elsewhere [18], we briefly detail the important points here, since the formation of the QDs critically depends upon the growth technique.

After planarization of the GaAs substrate and growth of a low temperature buffer layer, the active layers are deposited by migration-enhanced epitaxy. Initially, a ZnSe buffer layer of  $\sim 2.4$  nm is deposited followed by the ZnTe-Zn active layer. Preferential migration results in clus-

tering of Te-atoms, and eventually the formation of ZnSeTe QDs. The resulting 0.7 nm QD containing layer is then capped by a 2.4 nm ZnSe barrier. This process is repeated 240 times.

To understand the origin of QD formation in this multilayer superlattice structure, it is necessary to describe how certain characteristic features of the photoluminescence (PL) are related to the structure of the sample. The PL at 4 K is presented in Fig. 1. The observed PL displays the well-known two band behavior of the ZnSeTe system [19–21]. The shoulder around 2.6–2.75 eV (B) is generally accepted to be the result of recombination from excitons bound to pairs of Te-atoms [18,21], which substitute isoelectronically for Se [22]. The feature at  $\sim 2.79$  eV (C) is related to free excitons in the alloyed Zn(Te)Se matrix [18], while the dominant feature around 2.5 eV (A) has been historically attributed to the contribution of clusters of larger numbers of these isoelectronic centers. However, recently it has been shown that these Te-clusters evolve into type-II QDs in ZnTe/ZnSe structures if the Te deposition exceeds  $\sim 3$  MLs [23,24]. That process for the formation of QDs in the sample described in this Letter was recently confirmed by time-resolved PL measurements [23,25]. Furthermore, it has also been shown that the QDs, which evolve from the clustering of Te-atoms in the ZnTe/ZnSe multilayer structure described here, also align vertically and therefore form columnar QD-like nanostructures [14]. This configuration is shown schematically in the inset to Fig. 2(b). In such structures, the electron is not only bound to the hole via Coulomb attrac-

tion but is “forced” to align laterally beside the confined hole, creating a particularly suitable geometry for the observation of *AB* interference since the motion is forced to be in-plane by the geometry [8,11].

The inset in Fig. 1 shows a schematic model of the orbital motion of particles comprising such a localized exciton. In type-II Zn(Se)Te QDs, the hole is strongly confined by the nanostructure potential. As was demonstrated theoretically in Ref. [14], the electron in an exciton in a single Type-II QD is localized either above or below the QD, and no *AB* effect is expected. Thus, the *columnar* geometry of the system is of particular importance, since it dictates the ringlike geometry of the electron motion about the axis of the column. In addition, numerical calculations [14] show that the tunnel coupling between QDs in a stack is very weak, and an exciton cannot move in the *z* direction.

Based on the preceding discussion, we assume that an individual exciton is localized in one of the stacked QDs. Due to their radial spatial separation, the electron and hole form a rotating dipole with the two charged particles circumscribing orbits of different area. To obtain more

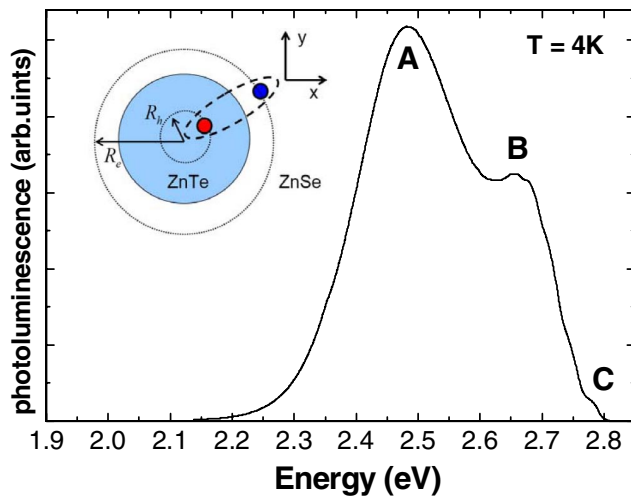


FIG. 1 (color online). PL of the ZnTe/ZnSe structure at 4 K. The contribution of the ZnSeTe QDs (A) and isoelectronic centers (B) are labeled. The emission from free excitons in the Zn(Te)Se matrix is also evident at 2.79 eV (C). The inset shows a schematic of the orbital motion of particles inside a localized exciton. The *x* and *y* axes belong to the cross-sectional plane. The trajectories of the bound electron and hole are shown as dotted lines.

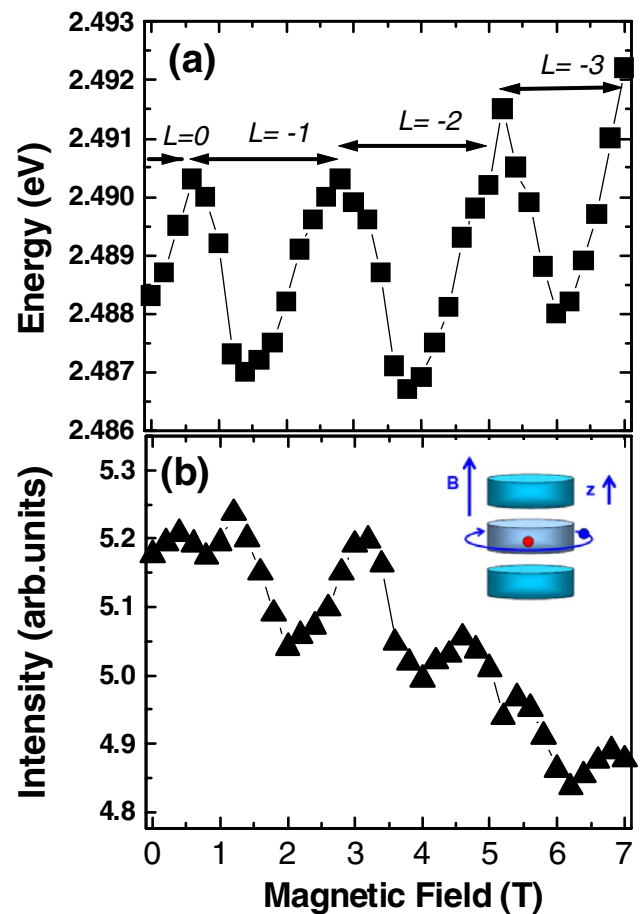


FIG. 2 (color online). Magneto-PL energy (a) and intensity (b) at 4 K for the ZnSeTe quantum dots (B).  $L = 0, -1, -2,$  and  $-3$  represent the transitions in total orbital momentum. Inset to Fig. 2(b) shows a schematic of the columnar QD geometry.

quantitative insight into this problem, we consider a simplified model, a rotating dipole in a magnetic field normal to the plane; the spectrum is given by [11]

$$E_{\text{exc}} = E_g + \frac{\hbar^2}{2MR_0^2} \left( L + \frac{\Delta\Phi}{\Phi_0} \right)^2, \quad (1)$$

where  $L$  is the angular momentum quantum number,  $E_g$  is the confined hole to electron ground state energy,  $\Phi_0 = hc/|e|$  is the magnetic flux quantum,  $R_0 = (R_e + R_h)/2$ , and  $M = (m_e R_e^2 + m_h R_h^2)/R_0^2$ . Here,  $R_h$  and  $R_e$  are the averaged radii of the orbits of the hole and electron, respectively, and  $m_h$  and  $m_e$  are their masses. The quantity  $\Delta\Phi = \pi(R_e^2 - R_h^2)B = 2\pi\Delta R \cdot R_0 B$  is the magnetic flux between the electron and hole trajectories (inset Fig. 1). The parameter  $\Delta\Phi/\Phi_0$  can be regarded as the AB phase. If we now assume that the hole is strongly localized inside the QD (i.e.,  $R_h = 0$ ), the average distance between electron and hole is just the radius of the electron orbit,  $\Delta R = R_e - R_h = R_e$ . According to Eq. (1), the rotating dipole shows a set of transitions between ground states with different  $L$ :  $L = 0 \rightarrow L = -1$ ,  $L = -1 \rightarrow L = -2$ , etc. Correspondingly, the energy of the lowest exciton state as a function of the magnetic field oscillates with the period  $\delta B = \Phi_0/\pi R_e^2$ . From the measured period of AB oscillations, we obtain  $R_e \approx 23.5$  nm, a reasonable value.

To determine the effects of magnetic field on the PL spectrum, the sample was mounted in the Faraday geometry, and the magneto-PL (MPL) was measured in 0.2 T steps. The energy and intensity of the two dominant features (A and B) were evaluated at each field through careful Gaussian fitting of the individual peaks. Below, we focus on the intensity and position of the peak A (ZnSeTe QDs), since the isoelectronic centers do not possess type-II geometry [14].

The effect of magnetic field upon the energy of the type-II ZnSeTe QDs (A) is shown in Fig. 2(a). Here, three well-resolved oscillations in the energy of the peak are evident; these oscillations are undamped over the magnetic field range studied. The effect of the magnetic field penetrating the ring upon the intensity of this peak is shown in Fig. 2(b). Again, clear oscillations are evident in the PL intensity, although the strength of these features is reduced.

Oscillations in the luminescence intensity due to coherent AB effects in QRs/QDs were first predicted by Govorov *et al.* [11], who showed that under the condition that the electron and hole are not strongly correlated, the simple picture described above is modified, and a periodic switching between a ground state transition with  $L = 0$ , to one with  $L \neq 0$ , will result with increasing magnetic field. Based on this picture, the Aharonov-Bohm phase in QD/QRs was suggested as a method to control the optical emission from nanostructures [11], since the PL lifetime and emission can be changed or controlled by an applied magnetic field to manipulate the AB phase.

The oscillations in the intensity of the PL shown in Fig. 2(b) suggests such behavior for the weakly bound electron and hole in type-II ZnSeTe QDs described here. However, the selection rules for transitions in total angular momentum are only strictly valid in the situation of perfect rotational symmetry. Here, it is highly probable that the ZnSeTe QDs are elongated; therefore, the selection rules may be relaxed allowing the observation of  $L \neq 0$  higher order states.

Although the exact origin of this behavior requires further study, until now this *switching* of the luminescence intensity has not been demonstrated in any AB system. This is significant because the modulation of the emission intensity is paramount if such processes are to be implemented in quantum information systems [15,16].

The effects of temperature are shown in Fig. 3. Figures 3(a) and 3(b) show the magnetic field dependence of the PL energy and intensity, respectively, for the ZnSeTe QDs at 60 K. With increasing temperature, the oscillations become less visible due to decoherence and fluctuations in the system. Nevertheless, as the inset to Fig. 3(a) shows, the AB effect is evident even at 180 K, which is now a viable temperature for application purposes. Above  $\sim 100$  K, the overall PL intensity, shown inset in Fig. 3(b), decreases rapidly with further increase of temperature. This is related

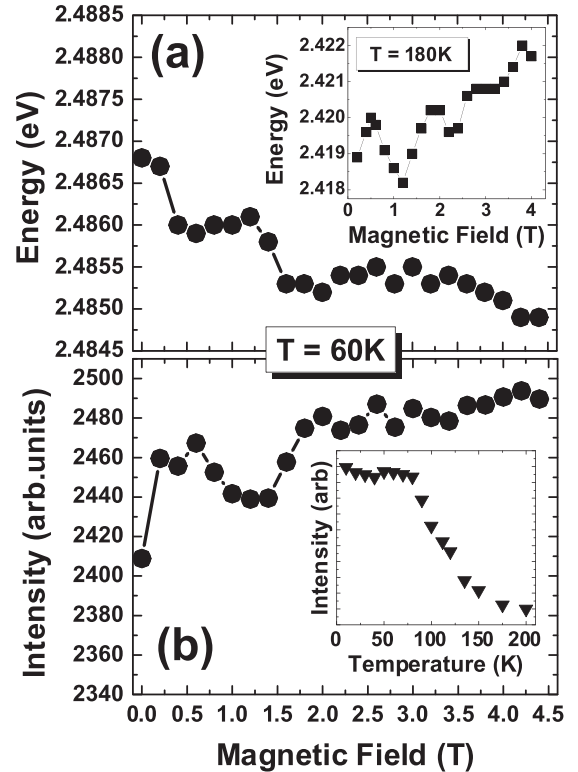


FIG. 3. Magneto-PL versus energy (a) and intensity (b) at 60 K for the ZnSeTe QDs. The inset to Fig. 3(a) shows the energy dependence at 180 K while the inset to Fig. 3(b) shows the temperature dependence of the integrated intensity of the dots.

to thermal ionization and is consistent with an exciton binding energy of 7.3 meV for these QDs [23].

In summary, we have observed unusually strong Aharonov-Bohm effects in both the intensity and energy of the PL of type-II ZnSeTe QDs. Furthermore, temperature studies reveal that the ABE in these type-II QDs is remarkably robust, persisting at temperatures up to 180 K. Although the subtleties of this behavior are not fully understood, the demonstration of coherence at high temperature indicates that type-II QD systems may be suitable for applications in quantum information processing.

We acknowledge support from DOE Grant No. DEFG02-05ER46219, BSC-CUNY Grant No. 68075-00 37 (I.L.K.), and the Center for Spin Effects and Quantum Information in Nanostructures (UB). One of the authors (A.O.G.) acknowledges support by the BioNano Technology Initiative at OU.

---

\*isellers@buffalo.edu

- [1] Y. Aharonov and D. Bohm, *Phys. Rev.* **115**, 485 (1959).
- [2] R.A. Webb, S. Washburn, C.P. Umbach, and R.B. Laibowitz, *Phys. Rev. Lett.* **54**, 2696 (1985).
- [3] G. Timp, A.M. Chang, J.E. Cunningham, T.Y. Chang, P. Mankiewich, R. Behringer, and R.E. Howard, *Phys. Rev. Lett.* **58**, 2814 (1987); C.J.B. Ford, T.J. Thornton, R. Newbury, M. Pepper, H. Ahmed, D.D. Peacock, R.A. Ritchie, and J.E.F. Frost, *Appl. Phys. Lett.* **54**, 21 (1989).
- [4] A. Fuhrer, S. Lüscher, T. Ihn, T. Heinzl, K. Ensslin, W. Wegscheider, and M. Bichler, *Nature (London)* **413**, 822 (2001); E.B. Olshanetsky, Z.D. Kvon, D.V. Sheglov, A.V. Latyshev, A.I. Toropov, and J.C. Portal, *JETP Lett.* **81**, 625 (2005).
- [5] A. Lorke, R.J. Luyken, A.O. Govorov, J.P. Kotthaus, J.M. Garcia, and P.M. Petroff, *Phys. Rev. Lett.* **84**, 2223 (2000).
- [6] N.A.J.M. Kleemans, I.M.A. Bominaar-Silkens, V.M. Fomin, V.N. Gladilin, D. Granados, A.G. Taboada, J.M. Garcia, P. Offermans, U. Zeitler, P.C.M. Christianen, J.C. Mann, J.T. Devreese, and P.M. Koenraad, *Phys. Rev. Lett.* **99**, 146808 (2007).
- [7] A.V. Chaplik, *Pis'ma Zh. Eksp. Teor. Fiz.* **75**, 343 (2002). [*JETP Lett.* **75**, 292 (2002)].
- [8] A.V. Kalameitsev, A.O. Govorov, and V.M. Kovalev, *JETP Lett.* **68**, 669 (1998).
- [9] K.L. Janssens, B. Partoens, and F.M. Peeters, *Phys. Rev. B* **64**, 155324 (2001).
- [10] M. Grochol, F. Grosse, and R. Zimmermann, *Phys. Rev. B* **74**, 115416 (2006).
- [11] A.O. Govorov, S.E. Ulloa, K. Karrai, and R.J. Warburton, *Phys. Rev. B* **66**, 081309(R) (2002).
- [12] M. Bayer, M. Korkusinski, P. Hawrylak, T. Gutbrod, M. Michel, and A. Forchel, *Phys. Rev. Lett.* **90**, 186801 (2003).
- [13] E. Ribeiro, A.O. Govorov, W. Carvalho, Jr, and G. Medeiros-Ribeiro, *Phys. Rev. Lett.* **92**, 126402 (2004).
- [14] I.L. Kuskovsky, W. MacDonald, A.O. Govorov, L. Muroukh, X. Wei, M.C. Tamargo, M. Tadic, and F.M. Peeters, *Phys. Rev. B* **76**, 035342 (2007).
- [15] N. Gisin, G. Ribordy, W. Tittel, and H. Zbinden, *Rev. Mod. Phys.* **74**, 145 (2002).
- [16] E. Knill, R. LaFlamme, and G. Milburn, *Nature (London)* **409**, 46 (2001).
- [17] A. Bachtold, C. Strunk, J.-P. Salvetat, J.-M. Bonard, L. Forró, T. Nussbaumer, and C. Schönenberger, *Nature (London)* **397**, 673 (1999).
- [18] I.L. Kuskovsky, C. Tian, G.F. Neumark, J.E. Spanier, I.P. Herman, W.-C. Lin, S.P. Guo, and M.C. Tamargo, *Phys. Rev. B* **63**, 155205 (2001).
- [19] V. Akimova, A.M. Akhekyan, V.I. Kozlovsky, Y.V. Korostelin, and P.V. Shapin, *Sov. Phys. Solid State* **27**, 1041 (1985).
- [20] Q. Fu, D. Lee, A.V. Nurmikko, L.A. Kolodziejcki, and R.L. Gunshor, *Phys. Rev. B* **39**, 3173 (1989).
- [21] A. Muller, P. Bianucci, C. Piermarocchi, M. Fornari, I.C. Robin, R. André, and C.K. Shih, *Phys. Rev. B* **73**, 081306(R) (2006).
- [22] M.D. Pashley, K.W. Haberern, W. Friday, J.M. Woodall, and P.D. Kirchner, *Phys. Rev. Lett.* **60**, 2176 (1988).
- [23] Y. Gu, I.L. Kuskovsky, M. van der Voort, G.F. Neumark, X. Zhou, and M.C. Tamargo, *Phys. Rev. B* **71**, 045340 (2005).
- [24] M. Jo, M. Endo, H. Kumano, and I. Suemune, *J. Cryst. Growth* **301–302**, 277 (2007).
- [25] M.C.-K. Cheung, I.R. Sellers, A.N. Cartwright, and B.D. McCombe, *Appl. Phys. Lett.* **92**, 032106 (2008).